EE247A Final Project: A Two-Legged MEMS Walking Microrobot

Xiaoer Hu[1], Chi Chung (Alvin) Li[2], Xiaosheng Zhang[1]
[1] *Department of Electrical Engineering and Computer Sciences, University of California, Berkeley*
[2] *Department of Mechanical Engineering, University of California, Berkeley*

***Abstract*—In this work, a two-legged MEMS walking microrobot was designed, simulated, fabricated, and tested. The standard two-mask SOI process was utilized for fabrication. This microrobot has in total 2 individually addressable legs with 12 pin-joints and driven by 4 inchworm motors. The total layout area is 100 mm², robot mass is 135 mg, and dimension is 6.8 mm long, 6.8 mm wide, and 7.5 mm tall. This walking microrobot can achieve 1 mm/s walking speed theoretically, with 500Hz applied electrical signals from external sources via wire connections.**

***Index Terms*—Microrobot, two-mask SOI process, electrostatic inchworm motor, silicon pin-joint**

I. Introduction

MILLIMETER to centimeter scale walking microrobots based on microelectromechanical systems (MEMS) have attracted great interests recently because of their small sizes, low power consumptions, and large versatilities. The actuation mechanisms for microrobots include external electric and magnetic fields, piezoelectric actuators, thermal actuators, and capacitive-coupling electrostatic motors [1], among which the electrostatic gap closing actuator (GCA) based angled-arm inchworm motor is chosen in this work because they are more energy-efficient, can provide large forces with long displacements, have high force-to-area densities, is easy to be fabricated by standard silicon processes, and can potentially be autonomously driven by on-board power source and control circuits without requiring external fields.

A previous work by D. Contreras et al. at UC Berkeley demonstrated a 1 mm/s speed six-legged walking microrobot based on the two-mask silicon-on-insulator (SOI) fabrication and chip-level assembly processes [2]. The reported microrobot is composed of two leg chips and one top hub chip, with several electrostatic inchworm motors to accumulate many small steps into one big move. Each of the six legs is actuated by two inchworm motors. The vertical axis motor has 1:1 mechanical advantage to the leg linkage to maximize the force applied to lift the robot itself, while the horizontal axis motor has 4:1 mechanical advantage to increase the moving speed. However, the large leg number makes the mechanical design and electrical signal routing complicated, and is costly in terms of total layout area, robot dimension and power consumption. Here, we propose a new walking microrobot design that only has two legs based on similar pin-joint linkage principles. Each of the legs is actuated by two electrostatic inchworm motors in vertical and horizontal directions. This design reduces the total layout area and body mass of the microrobot, and makes the electrical signal routing and assembly process easier compared to the six-legged design.

II. Robot Design

Planar microfabrication technologies on silicon or SOI wafers are widely used for MEMS devices. While 1 mm scale motion of microstructure can easily be achieved in the wafer plane, the motion is usually limited to 1 μm scale on the out-of-plane direction, which is far not enough for robot locomotion on the vertical direction. This disadvantage can be overcome by chip-level assembly of multiple planar fabricated chips to achieve large structure motion in all three directions. The chip-level assembly technology demonstrated in [1, 3] is used in this work to realize a three-dimensional microrobot composed of two leg chips and two top chips, shown in Figure 1 (a). The leg chips are held on vertical direction by the top chips, thus large-scale motion on both vertical and horizontal directions can be achieved. Figure 1 (b) shows a microscope image of the fabricated leg chip.

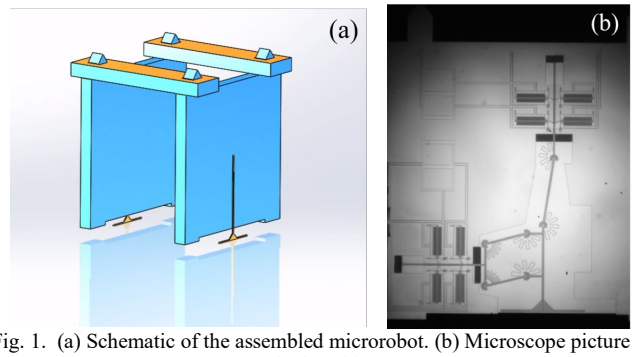

Fig. 1. (a) Schematic of the assembled microrobot. (b) Microscope picture of the leg chip.

A. Leg linkage design

Similar to the previous six-legged microrobot, each leg on this robot has to possess two degree-of-freedoms (DOF) to lift and push forward the robot independently. The horizontal and vertical motion of the leg is actuated separately by its own linear actuator (to be described in the next section). A four-bar linkage is designed to transmit these actuation force to the leg, shown in Figure 2 (a). The joints linking the beams together are silicon pin-joints with rotational springs, similar to the design in [4].

A parallelogram structure of bars are designed in the linkage such that the leg's orientation is fixed at all times to hold the robot strictly vertical. Note that although it is desirable to have the end point of the leg tracing straight loci (along the directions of actuation) while walking, the loci are slightly curved by design. This inevitable coupling between the two DOF are shown to be small in the simulation. A simulation of the linkage is shown in Figure 2(b) and Supplementary Video 1.

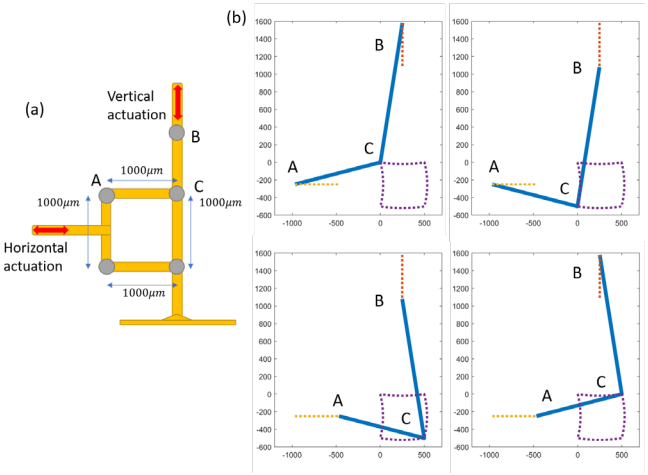

Fig. 2. (a) Leg linkage at center position (revolute joints are in grey). (b) Simulated locus of the leg linkage (simplified to three key joints) during an actuation cycle at four extreme positions. Length of AC section is 1000 μm and length of BC section is 1600 μm.

TABLE I
IMPORTANT DESIGN PARAMETERS OF THE INCHWORM MOTOR

Parameters	Numbers and Units
Estimated robot body mass (weight)	150 mg (1.4 mN)
Motor actuation voltage	100 V
Motor GCA actuation frequency	500 Hz
GCA finger overlap length	76.4 μm
GCA finger width	5 μm
GCA smaller gap	4.8 μm
GCA larger gap	7.75 μm
GCA max travel distance (defined by mechanical stopper)	3.8 μm
Number of gaps per GCA	60
GCA supporting spring stiffness	14.3 N/m
Minimum output force per GCA	1.96 mN
Approximated area per GCA	0.21 mm^2
Angled arm angle to the shuttle	64°
Angled arm critical force of buckling	24.7 mN
Shuttle minimum output force	1.8 mN
Shuttle total travel distance	500 μm
Shuttle supporting spring stiffness	0.27 N/m
Shuttle travel speed	2 mm/s
Power consumption per motor when being actuated	61 μW

B. *Electrostatic inchworm motor design*

Electrostatic GCA based angled-arm inchworm motor is used in the robot design to actuate the leg linkage in both directions. It is well known that electrostatic force between two parallel plates does not scale with respect to geometric dimensions and can be significantly larger than gravity or friction forces in small scale structures, therefore electrostatic actuators have played an important role in MEMS devices. However, electrostatic force is proportional to the inverse square of the gap width of two plates, thus limits the available actuation distance of an electrostatic actuator. In order to achieve both high output force and large actuation displacement, inchworm motor has been designed to accumulate hundreds of small GCA actuation steps to form a large travel using two sets of GCAs, where one of them actuates and locks the shuttle beam while the other one resets its position and prepares for the next actuation.

The principle of a GCA based angled-arm inchworm motor and its performance with respect to multiple design parameters has been thoroughly investigated and tested in [5, 6]. In general, the key points of design are (1) the available travel distance of GCA defined by the gap width and the mechanical stopper position should match the design of angled beam and shuttle teeth dimensions; (2) the total output force and shuttle travel distance should be enough for the designed robot leg motion (lifting the entire body up and moving forward); (3) the angled beam should not be buckled up when being actuated; (4) the force density, power consumption and resonant frequency of the motor should be optimized. The detailed design procedures are similar to those in [5] and thus not to be described in this paper. Some important design parameters and results are listed in Table I.

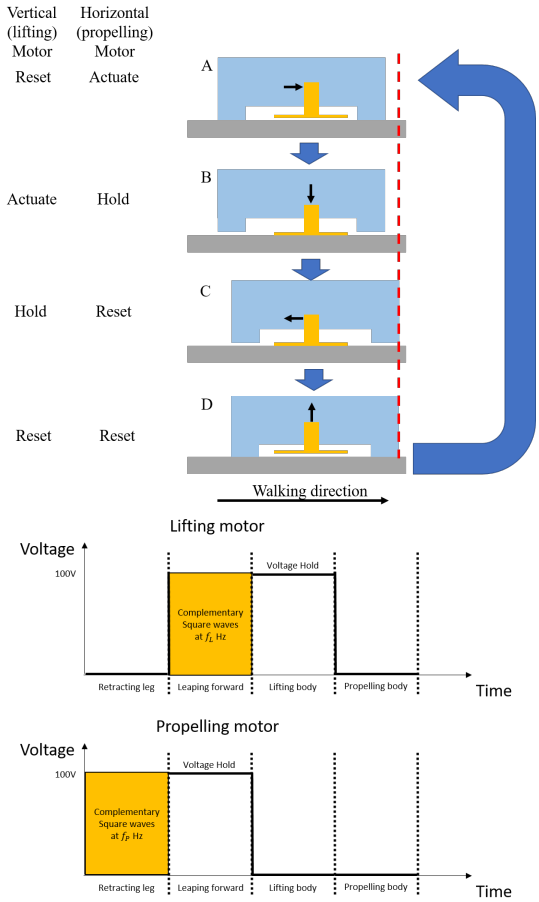

Fig. 3. Schematic of the microrobot walking gait and inchworm control signal time sequence. Actuate status: square waves are applied on two sets of GCA in an inchworm motor; Hold status: high voltage is continuously applied on one set of the GCAs in an inchworm motor and the shuttle is held in position; Reset status: voltages on two sets of GCA in an inchworm motor are both reset to 0 thus the shuttle position is reset by its supporting spring. Note that leg travel distance and body length are not in scale for a better view. Time of phase C and D is exaggerated in the figure for a better view, while in reality it is much shorter than time of A and B.

C. Electrical signal and walking gait

To demonstrate the walking microrobot principle and design, the microrobot in this work is controlled by electrical signals wired from external sources, though a fully autonomous microrobot requires onboard power source and control circuits. Each inchworm motor requires two signal connections and one ground connection, therefore at least 5 connections are required for each leg chip assuming two motors are commonly grounded. In this work, 5 wire bonding pads are designed on each leg chip for external signal connections, therefore totally 10 external wires are required. Electrical routing using the top chip as in [2] could be used to reduce the number of external wires to 5, however this increases the on-chip electrical routing and assembly process more complicated and thus is not used in this work.

The walking gait of the microrobot is shown in Figure 3. Legs on the two sides are actuated synchronously in a 4-phase fashion. In phase A the horizontal motors are actuated. In phase B the vertical motors are actuated and the robot body is lifted by legs. A "foot" is designed at the end of each leg thus the robot is stable when its body is lifted. In phase C the horizontal motors are reset and the robot body is moved forward, and then in phase D the vertical motors are also reset and the robot body touchs the ground again to start the next step.

III. Fabrication and Assembly

The robot is fabricated by a standard two-mask SOI process. From bottom to top, the wafer has 550 µm substrate silicon, 2 µm buried oxide, and 40 µm device silicon layer. The top device layer goes through standard photolithography process with the SOI mask, and the patterned photoresist becomes a mask for front side DRIE etch. Similarly, the bottom side substrate silicon layer is fabricated using the TRENCH mask. Finally, the chip is etched in HF vapor to release the moving parts. The design layouts are shown in Figure 4. Due to limited mask area for the entire class in this project, only one leg chip is actually fabricated.

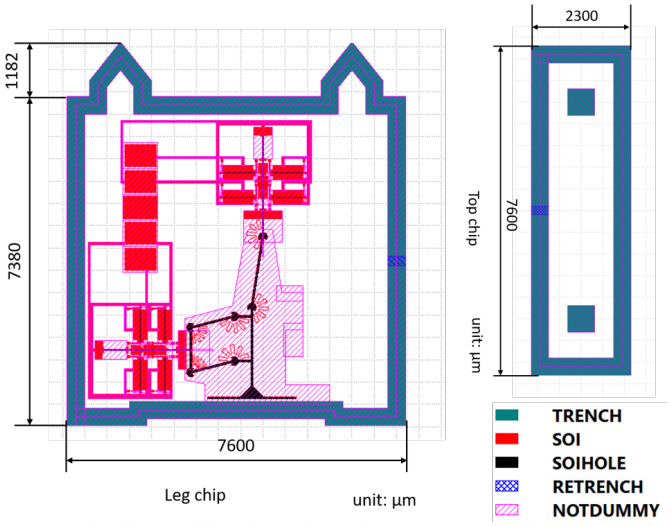

Fig. 4. Design layout of leg chip and top chip. DUMMY layer is not shown in the figures.

IV. Experimental Results

The motion of the designed robot leg is first qualitatively tested on a probe station. The electrical signal sequence shown in Figure 3 are applied via five probes to actuate the horizontal and vertical inchworm motors. The whole moving period of the leg with both vertical and horizontal motors biased captured by a microscope is shown in supplementary video 2. Figure 5 shows microscope images of the leg being actuated to several key positions. Despite a shuttle spring detached from its anchor, the robot leg is generally actuated as expected. However, when the horizontal and vertical inchworm motors are both actuated to its extreme position, the horizontal inchworm motor is not able to reset to its original position until the vertical inchworm motor is reset. This is mainly because the vertical force applied on the linkage results in a downward bending moment on the horizontal inchworm motor shuttle and thus locked the horizontal movement. The horizontal shuttle can only be retracted until the vertical force is removed. More detailed simulations on the mechanical properties of the linkage and better linkage designs are necessary to address this issue in the future.

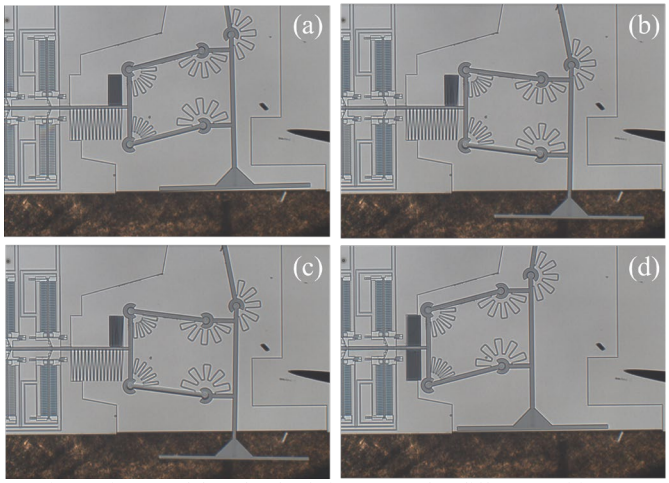

Fig. 5. Pictures of the robot leg being actuated at different positions, corresponding to the four phases in Fig. 3 except the horizontal shuttle fails to retract at phase C.

The actuation speed of the inchworm motors are then tested by applying electrical signals at different frequencies to the vertical motor while applying 0V to the horizontal motor. This test is only performed on the vertical motor since the design details for vertical and horizontal motors are the same, so the same electrical characteristics are expected from the two motors. Figure 6 shows the moving speed of the shuttle versus the frequency of applied voltage.

The designed shuttle moving step under each GCA actuation is 2 µm. Therefore, the theoretical moving speed of the motor is $v_{theoretical} = 2\times2\ \mu m\times f$, where f is the frequency of the applied square wave signal. The theoretical speed is plotted in Figure 6 in red dashed line. The blue solid line represents the real experimental results. From the plot, the relationship between the frequency and moving velocity is approximately linear. When the signal frequency is below 250 Hz, the experimental and theoretical speed match with each other very well. However, at high frequency, the

experimental speed is slower than the theoretical value, and the deviation grows linearly with frequency. This difference may be because at high frequency there are possible missing steps. Moreover, due to the limited frame rate of the camera (41.5 fps), the measured speed may be underestimated when the moving speed of the motor is high.

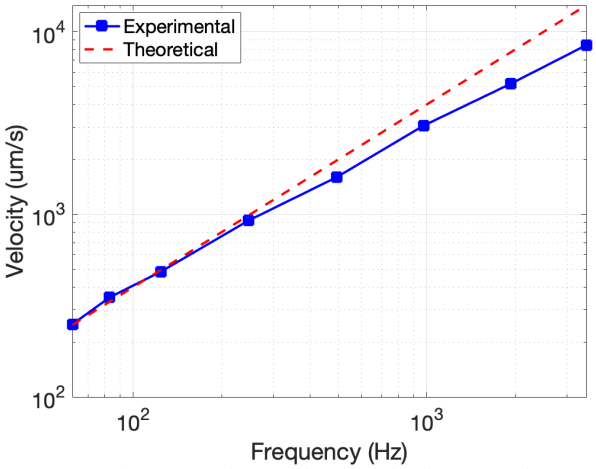

Fig. 6. Actuation speed vs actuation frequency plot.

V. Conclusions

In this paper, a design of two-legged MEMS walking microrobot is proposed, one of the leg chips is fabricated using a standard 2-mask SOI process, and the performance of the fabricated chip is tested. The locus and speed of the fabricated leg generally agree with the designed parameters. We believe the microrobot would be able to walk if both leg chips and top chips are fabricated, successfully assembled and electrically connected.

Some issues and potential improvements of the current design are observed during the experiments. (1) The vertical inchworm motor applies an obvious bending moment on the horizontal motor shuttle and prevents the horizontal motor from retraction, even when the robot body weight is not actually loaded on the leg. This suggests some forces and moments are possibly transferred by the joints due to friction and the rotational springs. Since friction cannot be totally avoided in the current pin-joint design, a possible solution is to re-design the shuttle and leg linkage to increase robustness against bending. (2) The electrical connection path of the horizontal motor is too close to the chip edge and thus can be easily damaged during fabrication and test. A re-design of electrical connections on the SOI device layer is necessary in the future version. (3) The shuttle holding springs tend to be easily detached from their anchors during the test. Also a detachment of angled beam on the inchworm motor is observed. Additional strengthening structures are necessary to make sure those points are not broken during operation. (4) Beams of the shuttle-serpentine spring tend to stick with each other when the inchworm motor is reset and the shuttle is retracted. Perhaps some mechanical stopper of bumper can be designed to prevent the spring beams from colliding with each other.

Besides improvements and more testing on the current two-legged microrobot design, we believe other principles of walking locomotion, such as walking based on vibration, can be further investigated and implemented in the future.

Acknowledgement

The authors thank Dr. Joseph Greenspun and Mr. Craig Schindler for tracking our design progress, providing useful suggestions, and fabricating the devices in UC Berkeley Marvel Nanofabrication Laboratory.

Supplementary Materials

Supplementary Video 1. Simulation of the leg linkage locus in an actuation cycle.
https://drive.google.com/open?id=15UKk0jw_wNJgpTpBK51S3LnQNE92W8lx

Supplementary Video 2. Experimental microscope video of the leg locus in an actuation cycle.
https://drive.google.com/open?id=1Al4UvnDx3OJpwYJQ84eLDu7bt8wRd_yf

References

[1] Daniel S. Contreras, Daniel S. Drew, and Kristofer S.J. Pister, "First steps of a millimeter-scale walking silicon robot," *19th International Conference on Solid-State Sensors, Actuators and Microsystems (TRANSDUCERS)*, IEEE, 2017.

[2] Daniel S. Contreras, and Kristofer S.J. Pister, "A six-legged mems silicon robot using multichip assembly," https://people.eecs.berkeley.edu/~pister/publications/2018/ContrerasHexapodMEMS2018.pdf

[3] Gaopeng Xue, Masaya Toda, and Takahito Ono, "Comb-drive xyz-microstage with large displacements based on chip-level microassembly," *Journal of Microelectromechanical Systems*, vol. 25, no. 6, pp. 989-998, 2016.

[4] Daniel S. Contreras, and Kristofer S.J. Pister, "Durability of Silicon Pin-Joints for Microrobotics," International Conference on Manipulation, Automation and Robotics at Small Scales (MARSS), IEEE, 2016.

[5] I Penskiy, and S Bergbreiter, "Optimized electrostatic inchworm motors using a flexible driving arm," *Journal of Microelectromechanical Systems*, vol. 23, no. 1, 015018, 2012.

[6] Daniel S. Contreras, and Kristofer S.J. Pister, "Dynamics of electrostatic inchworm motors for silicon microrobots," International Conference on Manipulation, Automation and Robotics at Small Scales (MARSS), IEEE, 2017.